The 7th International Supercritical CO_2 Power Cycles Symposium
February 21 – February 24, 2022, San Antonio, Texas
Paper 59

An improved off-design prediction model based on similarity analysis for turbomachinery under S-CO_2 Condition

Yongju Jeong
PhD student
KAIST
Daejeon, Korea

Seongmin Son
PhD student
KAIST
Daejeon, Korea

Seong Kuk Cho
PhD candidate
KAIST
Daejeon, Korea

Jeong Ik Lee
Professor
KAIST
Daejeon, Korea

ABSTRACT

Supercritical CO_2 (S-CO_2) power cycle is a variation of Brayton cycle. In contrast to the fact that Brayton cycle operates with a gas phase fluid, S-CO_2 power cycle operates with supercritical phase CO_2. Many advantages of S-CO_2 power cycle are rooted from the novel characteristics of supercritical state, including reduced compression work near the critical point. To observe the system behavior of S-CO_2 cycle, the off-design performances of compressor and turbine should be analyzed accurately. Off-design performances of turbomachinery are traditionally considered as a function of mass flow rate, rpm, inlet temperature and pressure. However, it is not practical to produce off-design performances according to these four variables due to an excessive amount of calculation. Instead, off-design performances are usually pre-calculated and represented as a performance map so that the performance can be shown with respect to mass flow rate and rpm while inlet temperature and pressure are fixed. The variation of temperature and pressure are converted into the variation of mass flow rate and rpm with the similitude concept. In this paper, the concept of similitude for off-design performance are illustrated. The applicability of five existing similitude models is evaluated for S-CO_2 compressor and turbine. Moreover, a modified model is proposed for off-design performance prediction of S-CO_2 compressor.

INTRODUCTION

Most of the power plants mainly have adopted a steam Rankine cycle or a gas Brayton cycle until now. Since the invention of energy conversion through a thermodynamic cycle, there has been always a great emphasis on energy source and power cycle to convert energy into useful work. At the same time, to devise a better power conversion cycle, various approaches were taken by researchers. One of the examples is an S-CO_2 (supercritical CO_2) Brayton cycle. An S-CO_2 power cycle operates with a supercritical fluid, where temperature and pressure of working fluid are above the critical point. Many advantages of S-CO_2 power cycle are rooted from its novel characteristics. The fluid has liquid like density, but at the same time, gas like low viscosity. Furthermore, the fluid properties near the critical point show dramatic changes and highly non-linear behavior. One particularly important thermodynamic property is the compressibility factor

and it is reduced greatly near the critical point [1]. Due to this reduced compression work, although S-CO_2 cycle utilizes compact turbomachinery like Brayton cycle, it has pump like minimized work similar to a steam Rankine cycle.

Since the S-CO_2 power cycle consists of various components such as compressor, turbine, and heat exchanger, it is clear that the off-design behaviors of each component determine the system level behavior. Among them, turbomachinery can have a great impact on the analysis due to the non-linear property changes of S-CO_2. Although performance prediction method for S-CO_2 compressor and turbine originated mainly from the method for air condition, S-CO_2 shows very strong real gas effects unlike air.

The off-design performances of turbomachinery are traditionally considered as a function of mass flow rate, rpm, inlet temperature and pressure. However, it is not practical to produce off-design performances according to these four variables, because it requires 4^{th} order calculation for every iteration in the system level analysis. Instead, the off-design performances for the design inlet conditions are usually pre-calculated and represented as a performance map. The performance is shown with respect to mass flow rate and rpm, and additionally variations of temperature and pressure are reflected by adopting the similitude concept. That is to say, it is possible to avoid calculations for each iteration in system analysis as well as to reduce 4^{th} order calculation to 2^{nd} order calculation. Several models have been developed for the off-design performance prediction and they are mostly for air conditions [2-6]. The validity of these methods for air condition is widely accepted due to large volume of experimental evidence. However, the applicability of such methods to S-CO_2 still needs to be investigated further.

In this paper, the concept of similitude models is briefly illustrated, and five existing similitude models from open literature are presented. To evaluate the prediction errors caused by the existing models, error quantification procedure is proposed using 1D mean-line code, KAIST-TMD. As a result, average and maximum prediction errors are obtained and summarized in this study. Moreover, the modification of an existing similitude model is conducted by relating density and the similitude of external loss effects to improve the prediction accuracy for S-CO_2 compressor.

SIMILITUDE CONCEPT FOR TURBOMACHINERY OFF-DESIGN PERFORMANCE PREIDCTION

The off-design performances of turbomachinery, generally measured by pressure ratio and efficiency, or enthalpy rise and efficiency, can be considered as a function of four variables, which are inlet temperature, inlet pressure, mass flow rate, and rpm. However, most of off-design performances are evaluated for different mass flow rate and rpm conditions while inlet temperature and pressure are fixed at the design conditions.

One can think that the off-design performance is a function, which has efficiency, pressure ratio, enthalpy rise as outputs, and operating conditions (temperature, pressure, mass flow rate, rpm), geometry, and fluid properties as inputs. An attempt to relate all of these variables to off-design performance will require an excessive amount of numerical simulations and experiments. Alternatively, researchers introduced dimensional analysis to reduce such complexity. Consequently, the non-dimensional groups are derived and the function can be simplified. There are several existing models. The differences among the models are how each model treats real gas effect deviating from ideal gas.

The simplest model is ideal gas model (IG) [2]. The relation among input and outputs can be expressed as shown in equation (1)

$$\mathrm{fn}(D, N, \dot{m}, P_{in}, T_{in}, R, \gamma, \mu) = P_{out}, T_{out}, \Delta H \quad (1)$$

In an attempt to simplify this relation, it is natural to introduce the dimensional analysis (Buckingham Pi theorem). Then this yields six dimensionless quantities. Since a geometry is fixed, regarding off-design performance, the diameter can be omitted. Furthermore, Reynolds number normally has little impact on performance except for very low Reynolds number flow, so removing Reynolds number from the function is also reasonable. As a result, the variables are simplified to five parameters as shown in equations (3)-(7). One of these parameters is temperature ratio. Temperature ratio can be converted into efficiency through equation (2). Consequently, equation (1) can be simplified to equation (8) with the derived five parameters.

$$\eta = \frac{T_{out,isen} - T_{in}}{T_{out} - T_{in}} = \frac{\left(\frac{P_{out}}{P_{in}}\right)^{(\gamma-1)/\gamma} - 1}{\left(\frac{T_{out}}{T_{in}}\right) - 1} \quad (2)$$

$$\Pi_1 = \frac{\dot{m}\sqrt{\gamma R T_{in}}}{\gamma P_{in}} \quad \text{; Flow parameter} \quad (3)$$

$$\Pi_2 = \frac{N}{\sqrt{\gamma R T_{in}}} \quad \text{; Speed parameter} \quad (4)$$

$$\Pi_3 = \frac{P_{out}}{P_{in}} = PR \quad \text{; Pressure ratio} \quad (5)$$

$$\Pi_4 = \frac{\Delta H}{\gamma R T_{in}} \quad \text{; Head parameter} \quad (6)$$

$$\Pi_5 = \frac{T_{out}}{T_{in}} \rightarrow \eta \quad \text{; Efficiency} \quad (7)$$

$$\mathrm{fn}\left(\frac{\dot{m}\sqrt{\gamma R T_{in}}}{\gamma P_{in}}, \frac{N}{\sqrt{\gamma R T_{in}}}\right) = PR, \frac{\Delta H}{\gamma R T_{in}}, \eta \quad (8)$$

Equation (8) implies that if the two operating conditions have the same flow parameters and speed parameters, the performance variables on the right hand side are expected to be the same as well. Using these equalities, it is possible to derive corrected mass flow rate and corrected rpm as shown in equations (9) and (10).

$$\left(\frac{\dot{m}\sqrt{\gamma R T_{in}}}{\gamma P_{in}}\right)_{cor} = \left(\frac{\dot{m}\sqrt{\gamma R T_{in}}}{\gamma P_{in}}\right)_{off} \rightarrow \dot{m}_{cor} = \dot{m}_{off}\left(\frac{P_{in,cor}}{P_{in,off}}\right)\sqrt{\frac{T_{in,off}}{T_{in,cor}}}\sqrt{\frac{\gamma_{cor}}{\gamma_{off}}} \quad \text{; Corrected mass flow rate} \quad (9)$$

$$\left(\frac{N}{\sqrt{\gamma R T_{in}}}\right)_{cor} = \left(\frac{N}{\sqrt{\gamma R T_{in}}}\right)_{off} \rightarrow N_{cor} = N_{off}\sqrt{\frac{T_{in,cor}}{T_{in.off}}}\sqrt{\frac{\gamma_{cor}}{\gamma_{off}}} \quad \text{; Corrected rpm} \quad (10)$$

IG model assumes the working fluid follows the ideal gas law. However, real gas effects cannot be neglected in many cases. Thus, compressibility factor is added to model real gas effect accurately in IGZ model [4].

Since specific heat ratio does not greatly change in ideal gas case, specific heat ratio is assumed to be a constant in IG and BNI models. However, it is often required to cover the variation of specific heat ratio for a real gas case. For this reason, Glassman [5] introduced the analogy of a critical condition. From the isentropic flow relation, it is possible to take equations (11) and (12) assuming the critical condition (M=1).

$$\frac{P_{st}}{P_t} = \left(1 + \frac{\gamma-1}{2}M^2\right)^{-\gamma/(\gamma-1)} \rightarrow \frac{P_{cr}}{P_t} = \left(\frac{2}{\gamma+1}\right)^{\gamma/(\gamma-1)}, M = 1 \quad (11)$$

$$\frac{T_{st}}{T_t} = \left(1 + \frac{\gamma-1}{2}M^2\right)^{-1} \rightarrow \frac{T_{cr}}{T_t} = \left(\frac{2}{\gamma+1}\right), M = 1 \quad (12)$$

The relation between BNI [6] and Glassman models is very similar to that of IGZ and IG models. Although, the variation of specific heat ratio is reflected by introducing analogy of the critical condition, the real gas effect is not fully captured in the model. Therefore, to further improve the model, compressibility factor is applied to Glassman model for developing BNI model. In short, BNI model is Glassman model with compressibility factor included.

Starting from IG model, aforementioned models have been improved step by step reflecting the real gas effect using compressibility factor and specific heat ratio variation. Nonetheless, Pham [6] concluded that existing correction models cannot successfully accommodate the variation of properties of S-CO_2, and the correction model using isentropic exponent [7] instead of specific heat ratio should be further utilized for the correction model.

The relationship of the existing models is summarized in Figure 1, and their non-dimensionalized parameters are tabulated in Table 1.

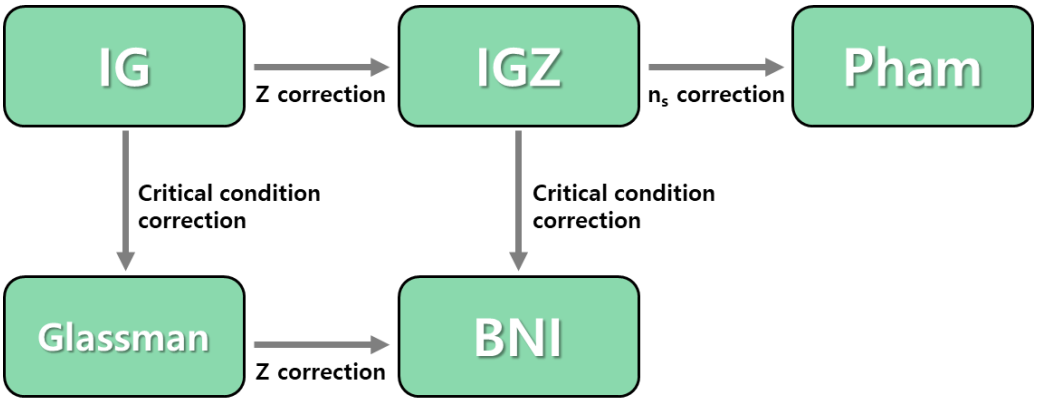

Figure 1. Flow chart of similitude model development [17]

Table 1. Summary of parameters for existing similitude models [18]

	Π_1	Π_2	Π_3	Π_4	Π_5
IG [3]	$\frac{\dot{m}\sqrt{\gamma RT}}{\gamma P}$	$\frac{N}{\sqrt{\gamma RT}}$	$\frac{\Delta H}{\gamma RT}$	PR	η
IGZ [4]	$\frac{\dot{m}\sqrt{\gamma ZRT}}{\gamma P}$	$\frac{N}{\sqrt{\gamma ZRT}}$	$\frac{\Delta H}{\gamma ZRT}$		
Glassman [5]	$\frac{\dot{m}\sqrt{\gamma RT_{cr}}}{\gamma P_{cr}}$	$\frac{N}{\sqrt{\gamma RT_{cr}}}$	$\frac{\Delta H}{\gamma RT_{cr}}$		
BNI [6]	$\frac{\dot{m}\sqrt{\gamma ZRT_{cr}}}{\gamma P_{cr}}$	$\frac{N}{\sqrt{\gamma ZRT_{cr}}}$	$\frac{\Delta H}{\gamma ZRT_{cr}}$		
Pham [6]	$\frac{\dot{m}\sqrt{n_s ZRT}}{n_s P}$	$\frac{N}{\sqrt{n_s ZRT}}$	$\frac{\Delta H}{n_s ZRT}$		

ANALYSIS TOOL – KAIST-TMD

KAIST-TMD is a 1-D mean streamline code for design and performance prediction of turbomachinery, developed by KAIST research team [8, 9]. In the preliminary stage of designing a turbomachine, it can be challenging to generate the specified geometry and to predict its performance. To overcome this difficulty, 1-D mean streamline method has been applied. Even though a fluid path in a turbomachine has three-dimensional complexity, most of the fluid flows from inlet to outlet. Therefore, it is possible to represent three-dimensional fluid motion one-dimensionally with velocity triangles. By using velocity triangles, continuity and energy conservation equation are simplified. Equation (13) indicates continuity and equation (14), i.e. Euler turbomachinery equation, indicates kinetic energy gain caused by the rotation of an impeller.

$$h_{o2} - h_{o1} = U_2 C_{w2} - U_1 C_{w1} \tag{13}$$

$$\dot{m} = \rho(h_s, P_s) A V \tag{14}$$

Aforementioned description of working fluid assumes an ideal fluid flow without irreversibility, because the fluid behavior is represented as 1-D flow. In reality, there are various secondary flow effects which cannot be expressed with velocity triangles and these cause irreversibilities. To reflect these irreversibilities, loss models should be applied to the 1-D mean streamline method. By considering this 1-D mean streamline method with loss models, the compression or expansion process can be described correctly in all conditions.

Because of aforementioned irreversibilities, it is very important to select a proper loss model set. In other words, the accuracy of performance prediction of 1-D mean streamline method heavily relies on loss models. Many institutions and companies have developed their own 1-D mean streamline codes for the design and performance prediction. KAIST-TMD is one of the developed codes. The compressor module was validated with Korea Atomic Energy Research Institute (KAERI) [10] and Sandia National Lab experimental data [11], and the turbine module was compared to NASA air turbine data using equivalent condition [12].

PREDICTION ERROR QUANTIFICATION PROCEDURE

In order to evaluate the accuracy of various similitude models, it is necessary to utilize a wide range of operation data. However, the number of S-CO_2 turbomachine operation data is very limited in the open literature to perform a quantified evaluation and generalize the results. Alternatively, it is possible to generate data with the simulation using 1-D mean streamline code. Thus, the generated data from KAIST-TMD was used for this study.

The outline to evaluate the accuracy of similitude models is presented in Figure 2. The process for the evaluation is as follows.

1. Generate performance data with respect to different mass flow rates and rpms at design point (temperature, pressure).

2. Prescribe the off-design temperature and pressure range, and choose one similitude model for evaluation.

3. Select one off-design operating condition, and calculate its performance.

4. Convert the off-design performance into corrected performance with the selected similitude model. One-to-one matching of mass flow rates and rpms between corrected data from off-design condition and reference data from design condition is imposed.

5. The inlet temperature and pressure are the same with the design condition due to the conversion. Then, if mass flow rates and rpms are the same, the performance of reference data and corrected data should be the same.

6. However, there will be discrepancy between the converted results and the reference. Therefore, the error can be quantified as mean absolute percent error (MAPE).

$$\text{MAPE} = \frac{100\%}{N} * \sum \left| \frac{Real\ value - Estimation}{Real\ value} \right| \tag{15}$$

7. Repeat the same procedure for other off-design conditions and similitude models.

By integrating all results within prescribed temperature and pressure range, it is possible to evaluate overall accuracy of the model and visualize the error distribution on the P-T plane. The example is shown in Figure 3. The red marker in the contour indicates design point, and the black marker indicates the analyzed off-design point. The black line in the performance map is off-design performance, but converted into design point. Accordingly, if the similitude model perfectly works, the two lines should overlap with each other. The errors are presented with colors in the contour.

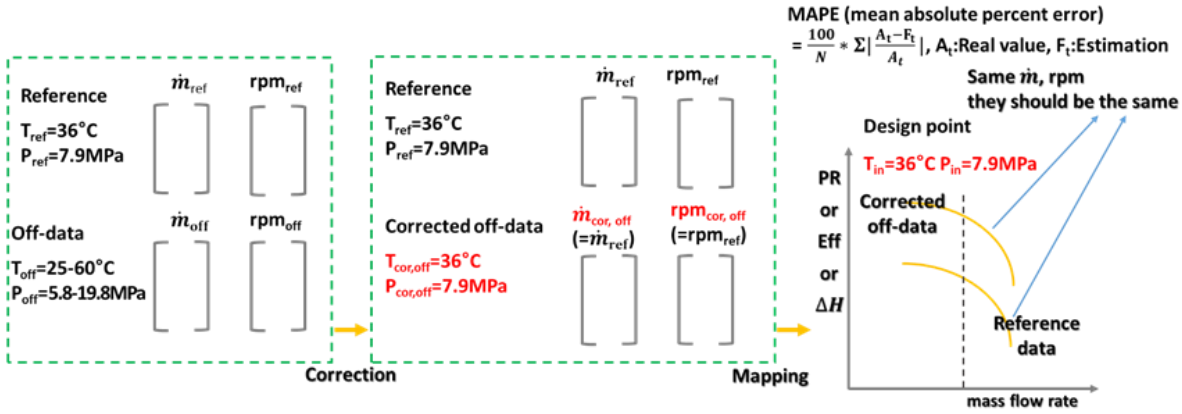

Figure 2. Flow chart of prediction error quantification procedure [17]

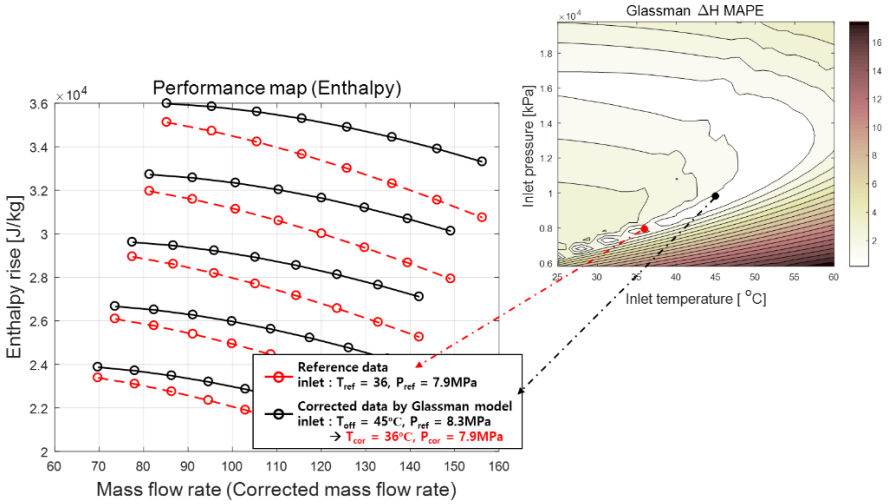

Figure 3. Example of error contour and comparison between reference and corrected performance data [17]

S-CO_2 TURBINE RESULTS

Table 2. S-CO_2 turbine design [18]

Design point			
T_{in}(°C)	500	ρ(kg/m^3)	253.24
P_{in}/P_{out}(kPa)	20000/8000	γ	1.5
m(kg/s)	129.15	Z	0.9
rpm(rev/min)	20000	n_s	1.44
Efficiency(%)	91.3		

Table 3. Studied inlet condition (S-CO_2 turbine)[18]

	Min	Max	Resolution
T(°C)	300	800	51
P(kPa)	5000	50000	226

Table 4. Average prediction error [%] (S-CO_2 turbine) [18]

Similitude model	PR MAPE	Eff MAPE	ΔH MAPE
IG	0.74	8.98	13.23
IGZ	3.47	0.27	0.79
Glassman	2.15	1.57	3.59
BNI	2.06	0.37	0.87
Pham	7.25	0.39	0.43

Table 5. Maximum pressure ratio prediction error [%] (turbine) [18]

Similitude model	MAPE (Max)
IG	3.92
IGZ	20.20
Glassman	11.03
BNI	10.60
Pham	50.65

Table 6. Maximum enthalpy rise prediction error [%] (turbine) [18]

Similitude model	MAPE (Max)
IG	35.30
IGZ	2.57
Glassman	10.7
BNI	2.10
Pham	1.58

Table 7. Maximum efficiency prediction error [%] (turbine) [18]

Similitude model	MAPE (Max)
IG	21.52
IGZ	0.80
Glassman	4.08
BNI	1.01
Pham	1.81

Above mentioned prediction error quantification procedure was conducted firstly for S-CO_2 turbine. The design condition of target turbine is presented in Table 2 and the range of off-design inlet condition was prescribed as shown in Table 3. The average and maximum errors of off-design performance prediction are summarized in Tables 4-7. Three performance indicators (pressure ratio, enthalpy rise, efficiency) were used for the evaluation. Thermodynamically, pressure ratio and enthalpy rise are interchangeable expression, but they should be distinguished for the similitude model. The detailed rationale will be mentioned in compressor result section. To begin with average prediction errors, most models show less than 10% prediction errors for pressure ratio, efficiency, and enthalpy rise in Table 4. For pressure ratio, IG model shows the best prediction capability. On the other hand, regarding enthalpy rise and efficiency prediction, IG model shows relatively poor accuracy and Pham model shows the best accuracy. Considering efficiency prediction accuracy, it would be better to choose the combination of efficiency and enthalpy rise prediction as performance indicators, instead of the combination of efficiency and pressure ratio. The maximum errors additionally support the use of efficiency and enthalpy rise. In Tables 5 and 6, although IG model shows the maximum error of 3.9% for pressure ratio, all the other models show the maximum errors above 10% for pressure ratio as well as the maximum error of IG model for efficiency prediction is over 30%. Therefore, it is recommended to use efficiency and enthalpy rise as performance indicators. Among the models, IGZ, BNI, and Pham models show good prediction capabilities, whose average prediction errors for efficiency and enthalpy rise are less than 1%. Their maximum errors are less than 3%.

S-CO_2 COMPRESSOR RESULTS

Table 8. Design condition summary (Comp1,2,3)

	Comp1	Comp2	Comp3
T_{in}(°C)	36.1	51	41
P_{in}/P_{out}(MPa)	7.9/20	9/20	14.6/25
m(kg/s)	129.2	129.2	129.2
rpm(rev/min)	15000	15000	15000
Efficiency(%)	78.7	73.8	82
ρ(kg/m^3)	329.4	276.7	767.3
γ	9	3.6	2.9
Z	0.41	0.53	0.32
n_s	1.54	1.49	8.9

Table 9. Range of studied inlet condition (S-CO_2 compressor)

	Min	Max	Resolution
T(°C)	25	60	36
P(MPa)	5.8	19.8	29

Table 10. Summary of average prediction error (Comp1) [MAPE, %] [17]

	PR	Eff	ΔH	PR from ΔH
IG	41.2	8.2	8.2	5.8
IGZ	43.9	8.3	7.6	5.5
Glassman	18.0	7.5	3.3	2.3
BNI	18.0	7.2	3.5	2.5
Pham	119.5	7.8	1.0	0.72

Table 11. Summary of average prediction error (Comp2) [MAPE, %]

	PR	Eff	ΔH	PR from ΔH
IG	30.1	17.0	2.2	1.4
IGZ	21.5	16.2	3.8	2.5
Glassman	19.3	14.9	1.5	1.0
BNI	11.2	16.6	3.5	2.4
Pham	100.1	12.0	0.46	0.30

Table 12. Summary of average prediction error (Comp3) [MAPE, %]

	PR	Eff	ΔH	PR from ΔH
IG	24.5	4.2	12.7	5.5
IGZ	18.0	1.8	3.6	1.6
Glassman	14.5	3.8	12.5	5.4
BNI	5.9	1.6	3.0	1.3
Pham	21.0	0.49	0.17	0.076

Table 13. Summary of maximum error of enthalpy rise prediction (Comp1,2,3) [MAPE, %]

	Comp1	Comp2	Comp3
IG	41.5	12.8	57.2
IGZ	10.6	6.0	13.7
Glassman	18.3	6.7	52.1
BNI	6.10	6.2	11.2
Pham	3.66	1.7	2.4

Table 14. Summary of maximum error of efficiency prediction (Comp1,2,3) [MAPE, %]

	Comp1	Comp2	Comp3
IG	41.2	59.4	28.3
IGZ	17.4	30.1	27.7
Glassman	46.6	56.8	26.0
BNI	18.7	48.0	8.9
Pham	16.6	27.5	2.0

Three compressors were designed to operate in the supercritical phase. Here, these compressors were named as Comp1, Comp2, and Comp3. Comp1 is a compressor operating near the critical point, and its operation is expected to have an influence by dramatic property changes of CO_2. Even though supercritical CO_2 does not have clear phase change between liquid and gas, there are regions where CO_2 behaves similar to either liquid or gas, and this region is divided by the pseudo-critical line (i.e. Willson line). Comp2 and Comp3 are

compressors designed in the liquid-like and gas-like regions, respectively. To observe the prediction errors and trends, off-design operation range was prescribed within 25-60°C and 5.8-19.8MPa for all compressors. The design points and off-design operating range are summarized in Tables 8-9.

In Tables 10-12, average prediction errors for pressure ratio and enthalpy rise are summarized. As mentioned above, pressure ratio and enthalpy rise are interchangeable thermodynamically. However, these two parameters are distinguished in the similitude model. This is because the similitude condition derived from dimensional analysis is not the same for pressure ratio and enthalpy rise. To be more specific, pressure ratio similitude is shown in equation (16).

$$\mathrm{PR_{cor}} = \mathrm{PR_{off}} \tag{16}$$

However, enthalpy rise similitude implies equation (17). Corrected enthalpy rise can be derived from equation (18), and it can be used to produce outlet enthalpy. Eventually, outlet pressure ratio can be derived with outlet enthalpy and constant entropy assumption between inlet and outlet through equations (18)-(21). Then, pressure ratio from equation (16) and pressure ratio from equation (21) can be compared. Since equations (16) and (17) indicate the two different similitude conditions, these two pressure ratios are not always the same.

$$\left(\frac{\Delta \mathrm{H}}{\gamma \mathrm{RT}}\right)_{\mathrm{cor}} = \left(\frac{\Delta \mathrm{H}}{\gamma \mathrm{RT}}\right)_{\mathrm{off}} \tag{17}$$

$$\Delta \mathrm{H_{cor}} = (\gamma \mathrm{RT})_{\mathrm{cor}} \left(\frac{\Delta \mathrm{H}}{\gamma \mathrm{RT}}\right)_{\mathrm{off}} \tag{18}$$

$$\mathrm{H_{out,isen}} = \mathrm{H_{in}} + \Delta \mathrm{H_{cor}} \tag{19}$$

$$\mathrm{P_{out}} = \mathrm{fn}(\mathrm{S_{in}}, \mathrm{H_{out,isen}}) \tag{20}$$

$$\mathrm{PR} = \mathrm{P_{out}}/\mathrm{P_{in}} \tag{21}$$

Since most of air condition follows the ideal gas law, it is reasonable to assume constant specific heat and its ratio as well. That is, head parameter can be rearranged into equation (25) through equations (22)-(24). In short, it is possible to relate head parameter and pressure ratio similitude under air condition. However, S-CO_2 shows dramatic property changes including specific heat and its ratio near the critical point, which makes it undesirable to use equation (25).

$$\frac{\mathrm{T_{out}}}{\mathrm{T_{in}}} = \left(\frac{\mathrm{P_{out}}}{\mathrm{P_{in}}}\right)^{(\gamma-1)/\gamma} \tag{22}$$

$$\mathrm{C_P} = \frac{\gamma \mathrm{R}}{\gamma - 1} \tag{23}$$

$$\Delta \mathrm{H} = \mathrm{H_{out}} - \mathrm{H_{in}} = \mathrm{C_P}(\mathrm{T_{out}} - \mathrm{T_{in}}) = \mathrm{C_P T_{in}} \left(\frac{\mathrm{T_{out}}}{\mathrm{T_{in}}} - 1\right) = \frac{\gamma}{\gamma - 1} \mathrm{RT_{in}} \left(\left(\frac{\mathrm{P_{out}}}{\mathrm{P_{in}}}\right)^{(\gamma-1)/\gamma} - 1\right) \tag{24}$$

$$\frac{\Delta \mathrm{H}}{\gamma \mathrm{RT_{in}}} = \frac{1}{\gamma - 1} \left(\left(\frac{\mathrm{P_{out}}}{\mathrm{P_{in}}}\right)^{(\gamma-1)/\gamma} - 1\right) = \mathrm{fn}(\mathrm{P_{out}}/\mathrm{P_{in}}) \tag{25}$$

In the last columns of Tables 10-12, derived pressure ratio prediction errors from enthalpy rise are presented to compare the accuracies of enthalpy rise prediction and pressure ratio prediction equivalently. The comparison indicates that enthalpy rise prediction significantly outperforms pressure ratio prediction in all models. This observation is compatible with the discussion through equations (16)-(25), which clarified the validity of constant specific heat ratio assumption.

Among the five existing models, Pham model shows the most accurate enthalpy rise prediction in average as shown in Tables 10-12. Besides average prediction errors, it is necessary to

observe local maximum errors. As a result of the error quantification procedure, not only the maximum errors of each model can be found as shown in Tables 13-14, but also the error contours can be visualized as in Figure 9. In Table 13, even considering maximum errors, Pham model has the most accurate prediction capability of less than 4% for enthalpy rise.

The efficiency prediction average errors are shown in Tables 8-10. In Comp1, the models have approximately 10% errors. Although BNI model shows the most accurate prediction, the differences against other models are not significant. The average prediction errors of Comp2 are larger than Comp1 in general. The most accurate model is Pham of 12% error, but only slightly better than other models. The results of Comp1 and Comp2 may imply that the prediction accuracy differences between the similitude models are not substantial. Comp3 has less than 5% errors in average for all models, and particularly Pham model shows less than 0.5% error.

One might think about 10% level errors are acceptable accuracy for average prediction. However, their maximum errors should be considered as shown in Table 14. It was mentioned that enthalpy rise should be used for performance prediction instead of pressure ratio, and Pham model for enthalpy rise prediction has the most accurate prediction capability among the models. Accordingly, the maximum error for efficiency prediction by Pham model should be discussed to choose which model is the most suitable for predicting compressor off-design performance under S-CO_2 condition. Comp3 shows only the maximum error of 2%. On the other hand, Comp1 and Comp2 show the maximum errors of 16.6% and 27.5%, respectively, which might result in substantial errors in system level analysis. Thus, efficiency prediction of Pham model will be modified in the next section.

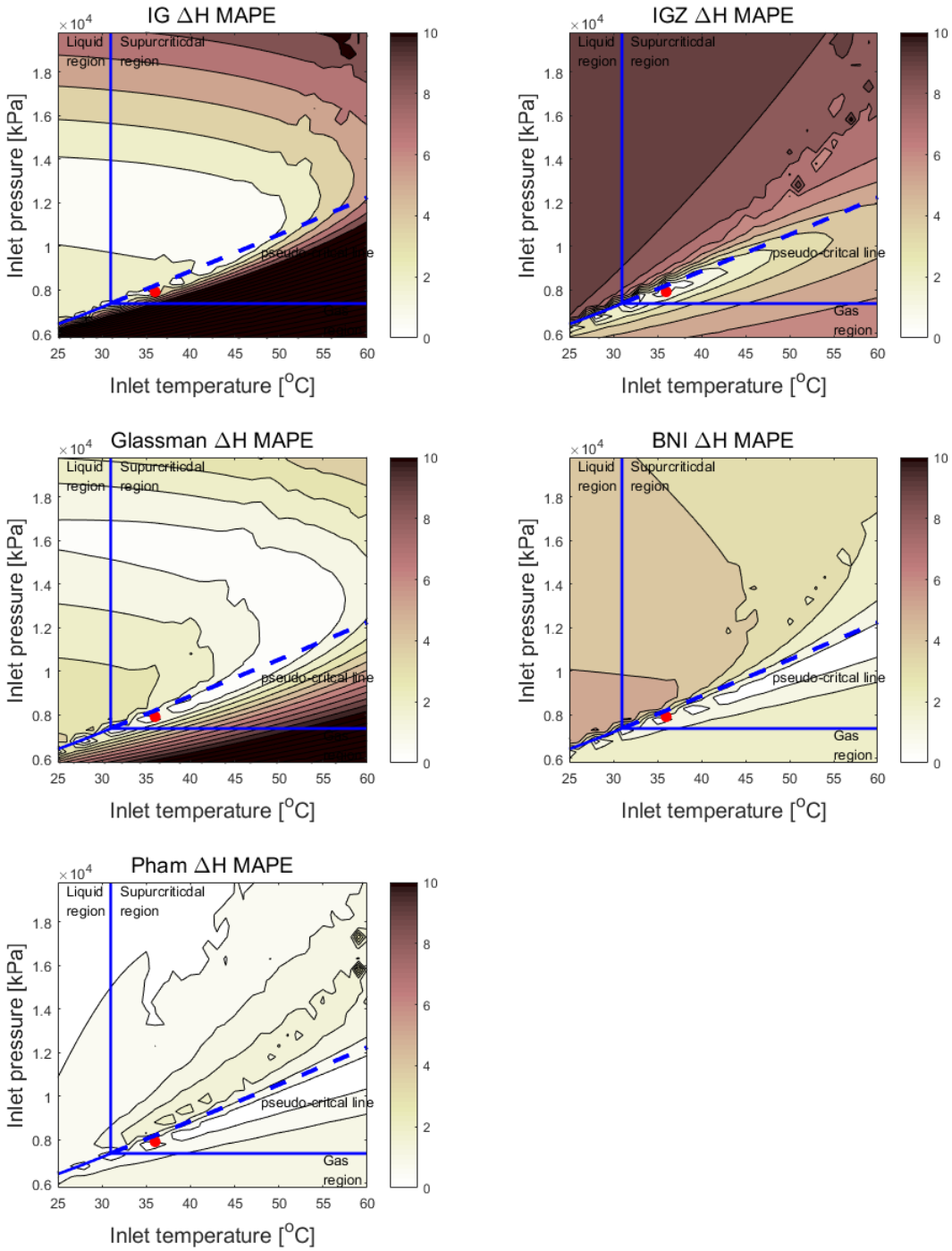

Figure 4. Enthalpy rise prediction error contours of Comp1 [%]

MODEL IMPROVEMENT BY DENSITY CORRECTION

Pham model shows the most superior performance prediction accuracy for S-CO_2 compressor off-design performance. Especially, enthalpy rise prediction was sufficiently accurate, whose average and maximum errors are below 1% and 5%, respectively. However, it appears that the

efficiency predictions by Pham model are not satisfactory, since 7.8% and 12% average errors occurs for Comp1 and Comp2, respectively. Moreover, the efficiency prediction of Comp1 shows the maximum error of 16.6%, and Comp2 shows the maximum error of 27.5%. The efficiency prediction error distributions of Pham model are shown in Figures 5, which show that the errors are mostly found in liquid-like region for Comp1 and Comp2. That is to say, Pham model fail to predict the efficiency, when a compressor is designed in the gas-like supercritical region but operates in the liquid-like supercritical region. Therefore, it is necessary to improve the accuracy of efficiency prediction in the liquid-like region.

In Figure 1, various correction methods are introduced such as using compressibility factor, adopting an analogy of critical condition, or using isentropic exponent. Likewise, similar correction method can be applied to improve the efficiency prediction of Pham model. The density distribution is overlapped as red line on the efficiency error contour in Figures 9 and 10, which points out that error distribution and density contour have a similar trend. This observation may imply that the correction using density can improve the prediction accuracy. It is also known that an S-CO_2 compressor has relatively large external loss effects in contrast to an air compressor due to high density of S-CO_2 in rotor cavity [11]. Therefore, inaccurate efficiency prediction was attributed to external loss effects in this study.

Since the enthalpy rise prediction of Pham model has an acceptable accuracy, only the improvement of efficiency prediction is presented in this section. It is found that previous studies also tried to modify efficiency prediction model. Glassman [5] suggested equation (26) to consider Reynolds number effect based on the viscous losses.

$$\frac{1-\eta_A}{1-\eta_B} = \left(\frac{Re_B}{Re_A}\right)^n, \text{ n=0.1~0.2} \tag{26}$$

On the other hand, Roberts [13] pointed out that importance of specific heat ratio on the efficiency prediction and proposed equation (27).

$$\frac{1-\eta_A}{1-\eta_B} = \left(\frac{\gamma_A}{\gamma_B}\right)^n, \text{ n=0.8} \tag{27}$$

These two studies both utilized efficiency as (1-η) in their formulations. (1-η) can be interpreted as the ratio between loss effect and ideal enthalpy rise. More specifically, it is possible to suggest equation (28).

$$\frac{1-\eta_A}{1-\eta_B} = \frac{\left(\frac{\Delta H_{loss}}{\Delta H_{id}}\right)_A}{\left(\frac{\Delta H_{loss}}{\Delta H_{id}}\right)_B} \tag{28}$$

Figure 6 displays loss effect composition changes with respect to backswept angle. Most compressors including air and S-CO_2 cases are usually designed to have the backswept angles ranging -50 ~ -60°, where leakage and disk friction loss constitute 30~40 percent of total loss effects. Accordingly, analytical simplification was imposed to figure out which loss does not satisfy the similitude among external losses. To begin with leakage loss, leakage loss effects between reference and off-design conditions can be expressed as in equation (29). KAIST-TMD adopts the leakage loss model suggested by Aungier [14], which consists of equations (30)-(32). During off-design operation, geometric information does not vary, so the original equations can be simplified to the last terms of equations (30)-(32). The similitude of Pham model gives equations (32)-(36). By combining the leakage loss model with the equalities from Pham model, equation (29) can be converted into equation (37), and this means similitude is satisfied in the leakage loss term.

$$\frac{1-\eta_{ref}}{1-\eta_{off}} = \frac{\left(\frac{\Delta H_{lk}}{\Delta H_{id}}\right)_{ref}}{\left(\frac{\Delta H_{lk}}{\Delta H_{id}}\right)_{off}} \tag{29}$$

$$\Delta P_{lk} = \frac{m(r_2 C_{w2} - r_1 C_{w1})}{Z' \bar{r}\, \bar{b} L_b} = \frac{m(\omega r_2 C_{w2} - \omega r_1 C_{w1})}{Z(\omega \bar{r}) \bar{b} L_b} \sim \frac{m \Delta H_{id}}{U} \tag{30}$$

$$U_{lk} = 0.816\sqrt{2\Delta P_{lk}/\rho} \sim m^{0.5} \Delta H_{id}^{0.5} U^{-0.5} \rho^{-0.5} \tag{31}$$

$$\Delta H_{lk} = \frac{\rho Z' \delta_{cl} L_b U_{lk} C_{w2} U_2}{m} \sim \frac{\rho U_{lk} U^2}{m} \sim \rho^{0.5} U^{1.5} m^{-0.5} \Delta H_{id}^{0.5} \tag{32}$$

$$a = \sqrt{n_s Z R T} \tag{33}$$

$$\frac{m\sqrt{n_s Z R T}}{n_s P} = \frac{m}{\rho a} \rightarrow \left(\frac{m}{\rho a}\right)_{off} = \left(\frac{m}{\rho a}\right)_{ref} \text{ ; Flow parameter} \tag{34}$$

$$\frac{N}{\sqrt{n_s Z R T}} = \frac{N}{a} \rightarrow \left(\frac{N}{a}\right)_{off} = \left(\frac{N}{a}\right)_{ref} \text{ ; Speed parameter} \tag{35}$$

$$\frac{\Delta H_{id}}{n_s Z R T} = \frac{\Delta H_{id}}{a^2} \rightarrow \left(\frac{\Delta H_{id}}{a^2}\right)_{off} = \left(\frac{\Delta H_{id}}{a^2}\right)_{ref} \text{ ; Head parameter} \tag{36}$$

$$\begin{aligned} \frac{1-\eta_{ref}}{1-\eta_{off}} &= \left(\frac{\Delta H_{lk,ref}}{\Delta H_{lk,off}}\right)\left(\frac{\Delta H_{id,off}}{\Delta H_{id,ref}}\right) \sim \left(\frac{\rho_{ref}}{\rho_{off}}\right)^{0.5} \left(\frac{U_{ref}}{U_{off}}\right)^{1.5} \left(\frac{m_{ref}}{m_{off}}\right)^{-0.5} \left(\frac{\Delta H_{id,off}}{\Delta H_{id,ref}}\right)^{0.5} \\ &\sim \left(\frac{\rho_{ref}}{\rho_{off}}\right)^{0.5} \left(\frac{a_{ref}}{a_{off}}\right)^{1.5} \left(\frac{\rho_{ref} * a_{ref}}{\rho_{off} * a_{off}}\right)^{-0.5} \left(\frac{a_{off}^2}{a_{ref}^2}\right)^{0.5} = 1 \text{ ; Similitude holds} \end{aligned} \tag{37}$$

Secondly, disk friction loss can be interpreted likewise above. Efficiency is connected to disk friction loss as shown in equation (38). The disk friction loss model [15] can be simplified as shown in equations (39)-(41) with fixed geometry during operation. By combining equations (34)-(36) with equations (39)-(41), equation (38) can be simplified as a function of density, viscosity, and sonic velocity. Moreover, the ratios of sonic velocity and viscosity do not change much in the liquid-like supercritical region as shown in Figure 7, so viscosity and sonic velocity effect can be neglected. The simplification results are shown in equation (42). In contrast to the leakage loss case, equation (42) yields the density ratio with the exponent of 0.2, and this does not satisfy the similitude suggested by Pham model. Therefore, inaccurate efficiency prediction of Pham model is likely to originate from the disk friction among external loss effects.

$$\frac{1-\eta_{ref}}{1-\eta_{off}} = \frac{\left(\frac{\Delta H_{df}}{\Delta H_{id}}\right)_{ref}}{\left(\frac{\Delta H_{df}}{\Delta H_{id}}\right)_{off}} \tag{38}$$

$$Re_{df} = \frac{\rho_2 U_2 r_2}{\mu_2} \sim \frac{\rho U}{\mu} \tag{39}$$

$$C_M = \left(\frac{k_s}{r_2}\right)^{0.25} \left(\frac{s'}{r_2}\right)^{0.1} \left(\frac{b_3}{s'}\right) Re_{df}^{-0.2} \sim Re_{df}^{-0.2} \sim \frac{\rho U}{\mu} \tag{40}$$

$$\Delta H_{df} = C_M \rho_2 r_2^2 \frac{U_2^3}{m} \sim Re_{df}^{-0.2} \rho \frac{U^3}{m} \sim \rho^{0.8} U^{2.8} m^{-1} \mu^{0.2} \tag{41}$$

$$\frac{1-\eta_{ref}}{1-\eta_{off}} = \left(\frac{\Delta H_{df,ref}}{\Delta H_{df,off}}\right)\left(\frac{\Delta H_{id,off}}{\Delta H_{id,ref}}\right) \sim \left(\frac{\rho_{ref}}{\rho_{off}}\right)^{0.8}\left(\frac{U_{ref}}{U_{off}}\right)^{2.8}\left(\frac{m_{ref}}{m_{off}}\right)^{-1}\left(\frac{\mu_{ref}}{\mu_{off}}\right)^{0.2}\left(\frac{\Delta H_{id,off}}{\Delta H_{id,ref}}\right)$$
$$\sim \left(\frac{\rho_{ref}}{\rho_{off}}\right)^{0.8}\left(\frac{a_{ref}}{a_{off}}\right)^{2.8}\left(\frac{\rho_{ref}}{\rho_{off}}\right)^{-1}\left(\frac{a_{ref}}{a_{off}}\right)^{-1}\left(\frac{\mu_{ref}}{\mu_{off}}\right)^{0.2}\left(\frac{a_{ref}}{a_{off}}\right)^{-1} \quad (42)$$
$$\sim \left(\frac{\rho_{ref}}{\rho_{off}}\right)^{-0.2}\left(\frac{\mu_{ref}}{\mu_{off}}\right)^{0.2}\left(\frac{a_{ref}}{a_{off}}\right)^{-0.2} \sim \left(\frac{\rho_{off}}{\rho_{ref}}\right)^{0.2} \text{ ; Similitude does not hold}$$

By applying similar formulation of equations (26) and (27) but with density ratio, it is possible to relate density with efficiency correction as shown in equation (43). The reference density is a known variable as it is the density at the design point. Off-design condition density can be derived from the compressor inlet temperature and pressure under the off-design operation. Off-design efficiencies are calculated from KAIST-TMD in this study. Therefore, the remaining undefined variable is an exponent n. If the exponent can be determined for equation (43), this equation can be used to predict the efficiency of an S-CO_2 compressor.

$$\frac{1-\eta_{ref}}{1-\eta_{off}} = \left(\frac{\rho_{off}}{\rho_{ref}}\right)^{n} \quad (43)$$

By assuming the reference efficiency and the corrected efficiency are the same, equation (44) is derived.

$$\frac{1-\eta_{cor}}{1-\eta_{off}} = \left(\frac{\rho_{off}}{\rho_{ref}}\right)^{n} \rightarrow \frac{1-\eta_{cor}}{1-\eta_{off}} = \left(\frac{\left(\frac{P}{ZRT}\right)_{off}}{\left(\frac{P}{ZRT}\right)_{ref}}\right)^{n} \rightarrow \eta_{cor} = 1-(1-\eta_{off})\left(\frac{P_{off}}{P_{ref}}\right)^{n}\left(\frac{Z_{ref}}{Z_{off}}\right)^{n}\left(\frac{T_{ref}}{T_{off}}\right)^{n} \quad (44)$$

Equation (44) gives the corrected efficiency, which should be the same with the reference efficiency. Figure 8 shows global error and local maximum error changes with the exponent n value changes. Both Comp1 and Comp2 have the exponent n that can reduce global and local maximum at the same time. Considering variations of global and maximum errors, exponent n was determined to have the value of 0.23. This exponent value is close to the exponent of 0.2 suggested in equation (42), which supports the discussion regarding the inaccurate efficiency prediction caused by external loss effects. The minor discrepancy between two exponents can happen because equations (37) and (42) are the outcomes of idealized analytical calculation. Eventually, efficiency error distributions are improved as shown in Figures 9 and 10 for Comp1 and Comp2. The average and maximum errors improvements are summarized in Table 16.

To generalize the value of exponent n and justify the density correction, four additional compressors were designed and tested with the suggested method. The design conditions of these compressors are summarized in Table 15. The performance predictions with the modified Pham model are recapitulated in Table 16. Efficiency prediction indicates less than 3% average prediction error and 7% maximum error at most. Before the modification, the Pham model had approximately 10% average error and locally maximum error of 27.5% regarding efficiency prediction. Therefore, the efficiency correction by density can improve its accuracy effectively.

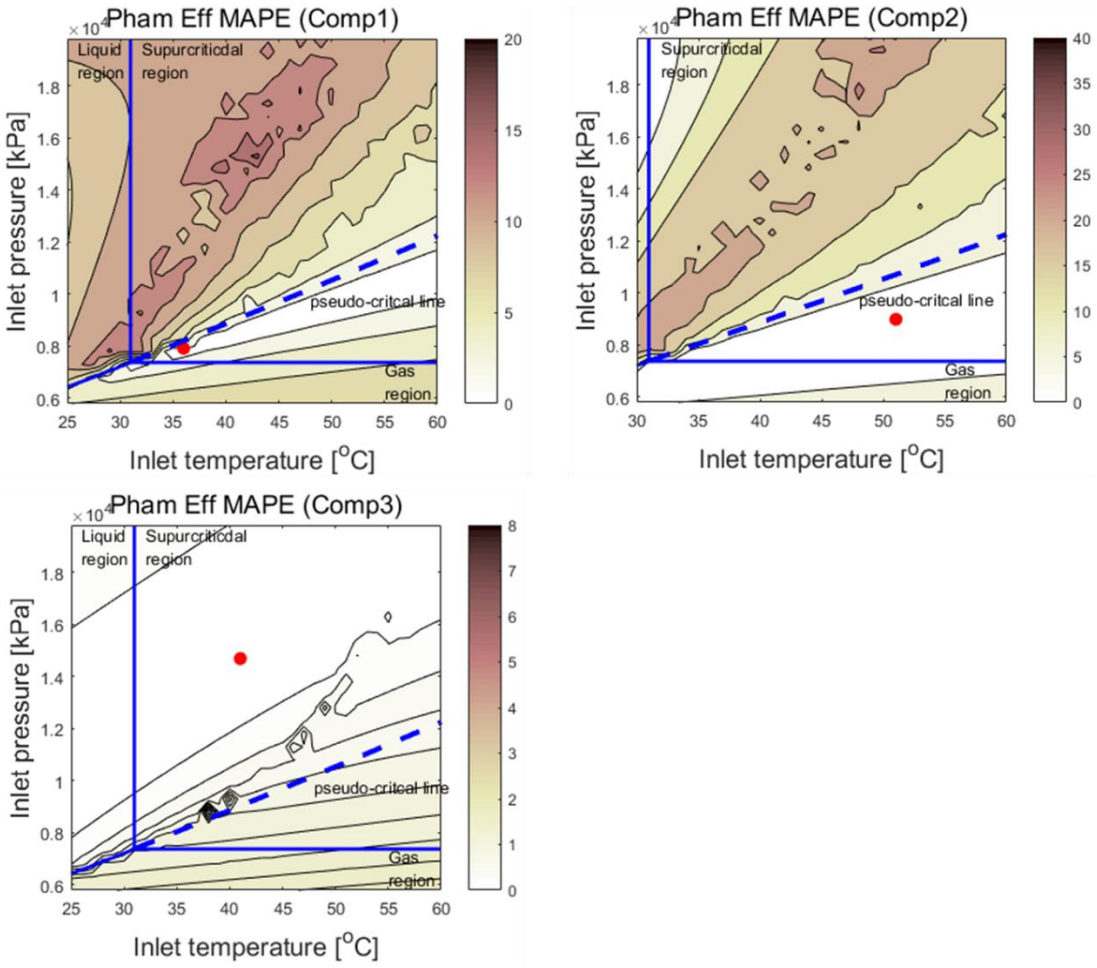

Figure 5. Efficiency prediction error contours of Pham model [%]

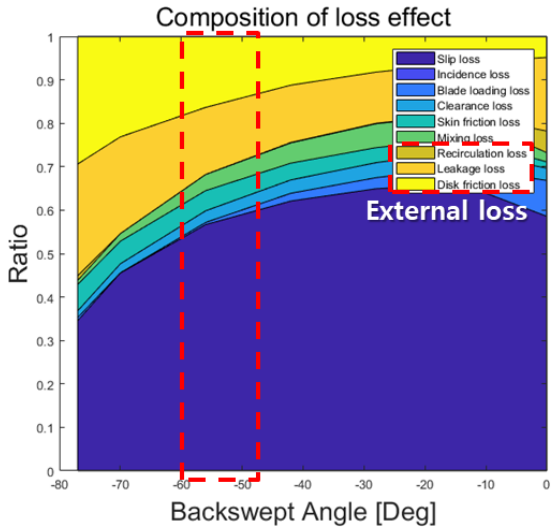

Figure 6. Loss effect composition changes according to backswept angle [16]

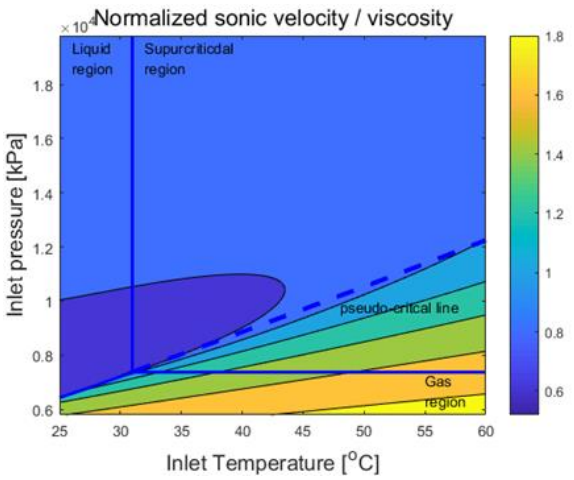

Figure 7. Variation of normalized sonic velocity/viscosity

Table 15. Design condition summary (Comp4, 5, 6, 7)

	Comp4	Comp5	Comp6	Comp7
T_{in}(°C)	43.3	55.3	56.7	45.0
P_{in}/P_{out}(MPa)	8.4/20	10/23	7.9/20	8.9/20
m(kg/s)	80	150	129.15	50
rpm(rev/min)	16000	13000	13000	15000
Efficiency(%)	75.3	74.7	74.3	71.0
ρ(kg/m^3)	287.7	322.5	195	324.8
γ	4.6	4	2.3	5.4
Z	0.48	0.5	0.65	0.46
n_s	1.5	1.6	1.35	1.6

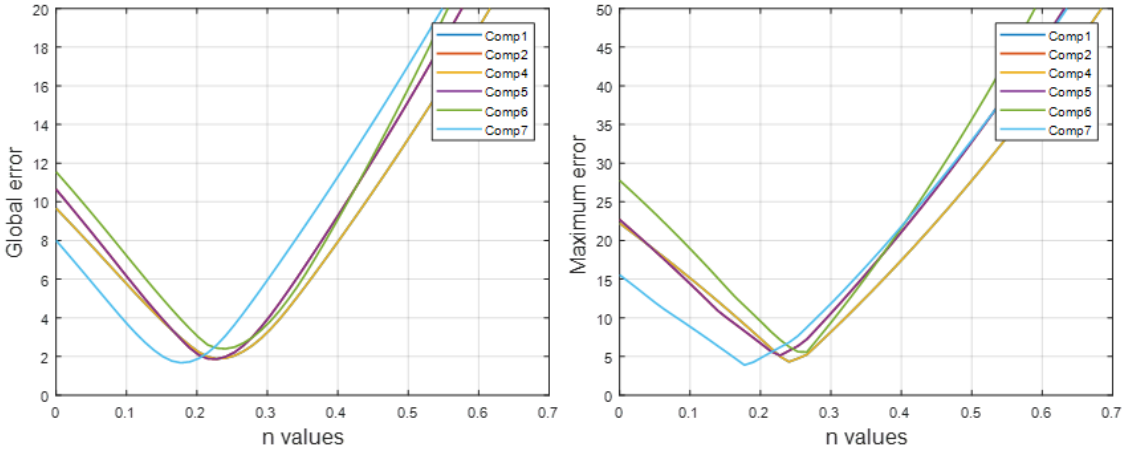

Figure 8. Variation of global and maximum errors according to n values (Efficiency prediction)

Table 16. Summary of performance prediction error by modified Pham model (n=0.23) [%]

	Average error			Maximum error		
	Enthalpy rise	Efficiency		Enthalpy rise	Efficiency	
	Pham (Modified Pham)	Pham	Modified Pham	Pham (Modified Pham)	Pham	Modified Pham
Comp1	1.0	7.6	1.6	3.7	16.6	5.0
Comp2	0.45	12.0	2.18	1.7	27.5	5.8
Comp4	0.56	9.7	1.88	2.1	22.2	4.9
Comp5	0.44	10.6	1.88	1.5	22.7	5.2
Comp6	0.61	11.6	2.42	2.6	27.8	7.0
Comp7	0.50	8.0	2.66	1.2	15.6	6.3

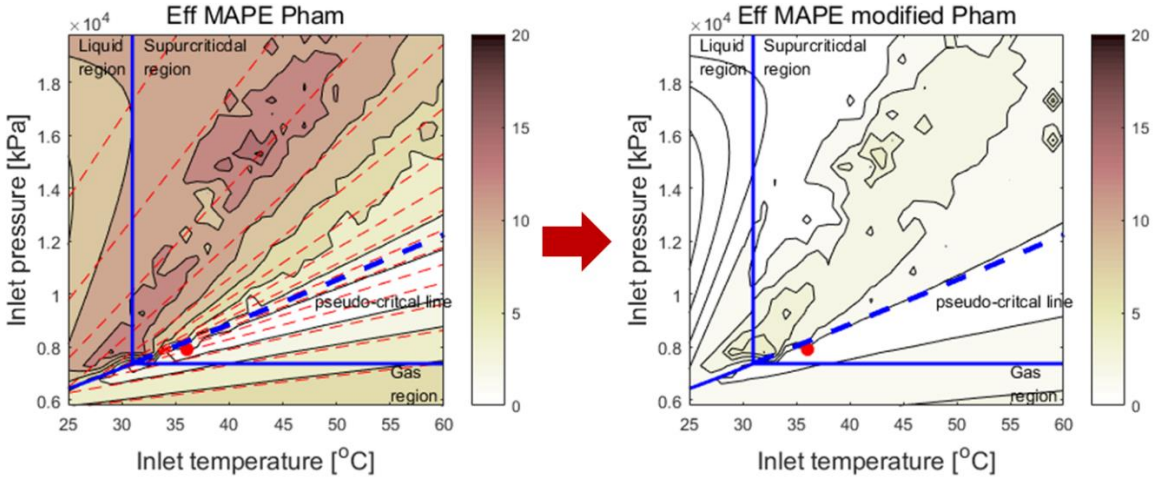

Figure 9. Efficiency correction by density in case of n=0.23 (Comp1)

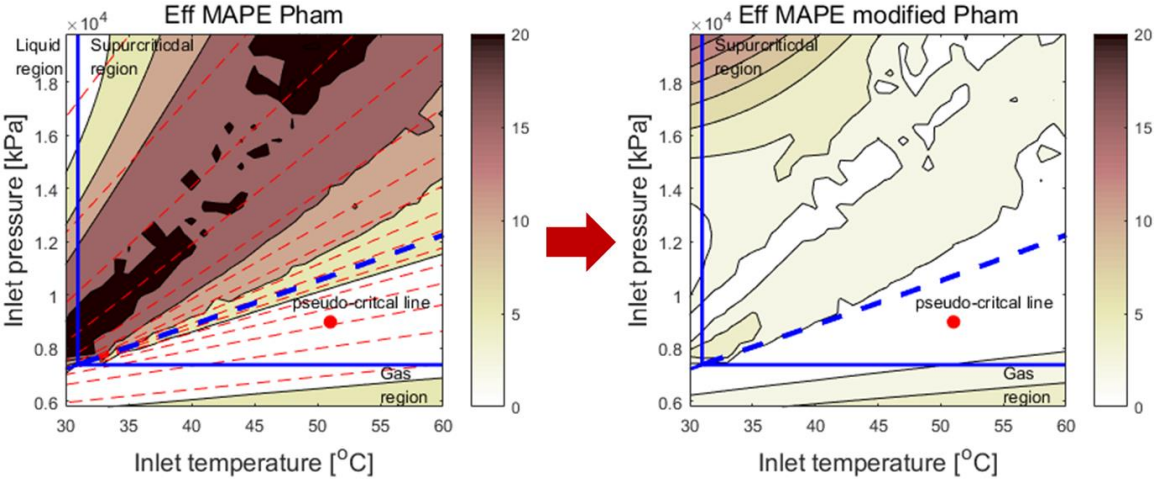

Figure 10. Efficiency correction by density in case of n=0.23 (Comp2) [%]

SUMMARY AND CONCLUSION

The off-design performances of compressor and turbine are conventionally presented in the form of a performance map, which represents performance indicator such as pressure ratio, enthalpy rise, and efficiency with respect to mass flow rate and rpm while inlet temperature and pressure are fixed. Although inlet temperature and pressure are fixed, it is possible to convert the temperature and pressure changes into the variation of mass flow rate and rpm with the similitude concept. Several models have been developed for the off-design performance prediction. However, the applicability of the existing models for S-CO_2 turbomachinery has not been extensively evaluated. Thus, the purpose of this paper is to evaluate the existing similitude models.

Due to the insufficient volume of experimental data in the open literature, KAIST-TMD was used to produce a large amount of data for the evaluation. Error quantification procedure was proposed and the accuracies of each model for S-CO_2 turbine and compressor were evaluated. As a result, average and maximum prediction errors were calculated as mean absolute percent error (MAPE). The existing similitude models for turbine can predict efficiency and enthalpy rise generally well. Among five models, IGZ, BNI, and Pham show good capabilities. In an S-CO_2 compressor case, Pham model shows the best prediction accuracy for enthalpy rise, but its maximum errors for efficiency prediction appears substantially large. Therefore, modification of Pham model was proposed in this paper for efficiency prediction, relating density to external loss effect in the view point of the similitude model.

NOMENCLATURE

A	Area
C	Absolute velocity
D	Impeller diameter
Eff	Efficiency
L_b	Blade length
M	Mach number
MAPE	Mean absolute percent error
N	rpm
P	Pressure
PR	Pressure ratio
R	Gas constant
Re	Reynolds number
S-CO_2	Supercritical carbon dioxide
T	Temperature
U	Impeller rotating velocity
V	Velocity
Z	Compressibility factor
Z`	Blade number

b	Blade height
h	Enthalpy
k_s	Frictional empirical parameter
m	Mass flow rate
n_s	Isentropic exponent
s	Entropy
s`	Disk gap
v	Specific volume
ΔH	Enthalpy rise
Π	Dimensionless or quasi dimensionless group
η	Efficiency
ρ	Density
μ	Viscosity
γ	Specific heat ratio
δ_{cl}	Tip clearance
ω	Rotating speed [rad/s]

Subscript

1	Impeller inlet
2	Impeller outlet
3	Diffuser inlet
a	Sonic velocity
cor	Corrected value
cr	Critical (sonic) condition
df	Disk friction
id	Ideal
in	Compressor inlet
isen	Isentropic process
lk	Leakage loss
m	Meridional direction
o	Total condition

off	Off-design condition
out	Compressor outlet
ref	Reference (design) condition
t	Total condition
w	Tangential direction

REFERENCES

[1] Dostal, Vaclav, Michael J. Driscoll, and Pavel Hejzlar. A supercritical carbon dioxide cycle for next generation nuclear reactors. Diss. Massachusetts Institute of Technology, Department of Nuclear Engineering, 2004.

[2] SARAVANAMUTTOO, Herbert IH; ROGERS, Gordon Frederick Crichton; COHEN, Henry. Gas turbine theory. Pearson Education, 2001.

[3] CUMPSTY, Nicholas A. Compressor aerodynamics. Longman Scientific & Technical, 1989.

[4] KIDNAY, Arthur J.; PARRISH, William R.; MCCARTNEY, Daniel G. Fundamentals of natural gas processing. CRC press, 2011.

[5] Glassman, A. J. (1972). Turbine design and application. nasa sp-290. NASA Special Publication, 290.

[6] PHAM, Hong-Son, et al. An approach for establishing the performance maps of the sc-CO2 compressor: Development and qualification by means of CFD simulations. International Journal of Heat and Fluid Flow, 2016, 61: 379-394.

[7] LÜDTKE, Klaus H. Process centrifugal compressors: basics, function, operation, design, application. Springer Science & Business Media, 2004.

[8] Lee, J., 2016. Study of improved design methodology of S-CO2 power cycle compressor for the next generation nuclear system application, Thesis, KAIST.

[9] Cho, Seong Kuk, et al. "S-CO2 Turbine Design for Decay Heat Removal System of Sodium Cooled Fast Reactor." ASME Turbo Expo 2016: Turbomachinery Technical Conference and Exposition. American Society of Mechanical Engineers, 2016.

[10] Cha, Jae Eun, et al. "Operation results of a closed supercritical CO2 simple Brayton cycle." The Fifth International Symposium—Supercritical CO2 Power Cycles. 2016.

[11] Wright, Steven A., et al. "Operation and analysis of a supercritical CO2 Brayton cycle." Sandia Report, No. SAND2010-0171 (2010).

[12] M. G. Kofskey, D. E. Holeski (1966). “Cold Performance Evaluation of a 6.02-Inch Radial Inflow Turbine Designated for a 10-Kilowatt Shaft Output Brayton Cycle Space power Generation System”, NASA TN D-2987

[13] ROBERTS, Stephen K.; SJOLANDER, Steen A. Effect of the specific heat ratio on the aerodynamic performance of turbomachinery. Journal of engineering for gas turbines and power, 2005, 127.4: 773-780.

[14] Aungier, R. H. Centrifugal Compressors: A Strategy for Aerodynamic Design and Analysis. 2000.

[15] Nemdili, A., & Hellmann, D. H. (2004). Development of an empirical equation to predict the disc friction losses of a centrifugal pump. In Sixth International Conference on Hydraulic Machinery and Hydrodynamics, Timisoara, Romania, Oct (pp. 21-22).

[16] Cho, Seong Kuk, et al. "Direction for High-Performance Supercritical CO2 Centrifugal Compressor Design for Dry Cooled Supercritical CO2 Brayton Cycle." Applied Sciences 9.19 (2019): 4057.

[17] Jeong, Yongju, et al. “A study of compressor off-design performance prediction with the similitude concept under supercritical CO2 Condition.” *15th Asian International Conference on Fluid Machinery, Busan, Korea*. 2019

[18] Jeong, Yongju, et al. " Similitude models for turbine off-design performance prediction under supercritical CO2 condition." *Transactions of the Korean Nuclear Society Fall Meeting, Goyang, Korea*. 2019.

ACKNOWLEDGEMENTS

This research was supported by Civil-Military Technology Cooperation Program (iCMTC) funded by the Agency for Defense Development – South Korea (17-CM-EN-04).